

Many-body aspects of the optical spectra of bulk and low-dimensional doped semiconductors

Andrei E. Ruckenstein

*Department of Physics, University of California at San Diego, La Jolla, California 92093
and Materials Research Branch, Naval Ocean System Center, San Diego, California 92152*

Stefan Schmitt-Rink

AT&T Bell Laboratories, Murray Hill, New Jersey 07974

(Received 12 September 1986)

We discuss the many-body aspects of the optical spectra of doped semiconductors, for both bulk and low-dimensional systems. At low doping concentrations the spectra are dominated by excitonic effects, consistent with the single-particle band structure of these systems. With increasing doping *atomic excitons* lose their identity and eventually unbind, while the spectral weight moves continuously to the Fermi level. Depending on the electron-mass to hole-mass ratio, the spectra display a broadened singularity as well as Auger-like indirect transitions. We calculate the onset of absorption in this regime to second order in the effective interaction. We stress that a calculation of the spectra near the Fermi level is outside the scope of conventional perturbation theory and we comment on the validity of various previously proposed calculational schemes. We conclude by discussing the problem in terms of Fadeev-like equations, which describe up to three-particle correlations exactly.

I. INTRODUCTION

In recent years, there has been renewed interest in the properties of one-component Coulomb systems in doped semiconductors. The main motivation for this interest is the increased ability of modern crystal-growth techniques to fabricate artificial structures, which (i) are of great technological importance, and (ii) provide controlled environments for studying conceptual aspects of quantum mechanics and many-body physics. Our work was motivated by luminescence experiments on optically pumped modulation-doped GaAs-Al_xGa_{1-x}As quantum wells (QW).¹ In these structures the carriers are spatially separated from the dopants, so that impurity scattering is minimized and the systems provide clean realizations of a (quasi-) two-dimensional Fermi gas, in which many-body effects can be more easily identified than in the bulk.

In a previous publication we gave a unified picture of optical processes in doped QW with particular attention paid to polarization anomalies observed in luminescence excitation spectra.¹ The main thesis of that work was that in doped semiconductors, and especially in doped QW, the collective behavior associated with the response of the Fermi sea in the course of excitation and emission processes is all important in determining the main features of the optical spectra. Similar conclusions have been drawn from recent luminescence experiments performed on QW waveguides.² (Observations of related effects have also been discussed in the context of highly excited semiconductors.³)

In the present article, we repeat in an extended form part of the discussion of Ref. 1 and we carry out the detailed calculation of Auger-like indirect optical transitions. As in Ref. 1, we stress that away from the indirect threshold, conventional perturbation theory fails and one

must appeal to new techniques. We argue that a calculation of the full spectra requires at least the solution of the three-particle problem as described by the Fadeev equations.⁴ Our discussion is, unless specified, independent of the dimensionality.

II. THE "RIGID" FERM SEA PICTURE

In the limit of small (or no) doping, the optical spectra of semiconductors close to the band gap display the usual atomic excitons—bound states of electrons and holes in the gap which form as a result of the attractive Coulomb interaction. The symmetry of these states is determined by the single-particle band structure of the system. With increasing doping concentration many-particle interactions lead to various effects on the spectra, which can be separated into *static* and *dynamic* ones.

We begin by considering the conventional "rigid" Fermi-sea picture in which the Fermi sea is not allowed to respond dynamically to the appearance or disappearance of the hole in the course of an optical transition. (For simplicity, throughout this paper we limit ourselves to *n*-type semiconductors, unless otherwise specified.) In this limit the many-body effects show up (i) as a static renormalization of the single-particle states and of the electron-hole interaction (static screening), and (ii) as a blocking of the available phase space as a result of the Pauli principle. Exchange and (static) correlation effects lead to a red shift of the band gap and, due to the partial cancellation of self-energy and vertex corrections, to a much weaker change in the absolute position of the exciton, resulting in a lowering of the exciton binding energy. Physically, this cancellation is a result of the charge neutrality of atomic excitons. When the doping concentration exceeds a critical value (the Mott density), the renor-

malized band gap falls below the exciton level so that atomic bound states are no longer stable.

It is worth mentioning that in one and two dimensions the main mechanism for the unbinding of atomic excitons (to be distinguished from the so-called “Mahan excitons”—see below) is different from that in three. In three dimensions the existence of a bound state requires a finite attractive interaction and the unbinding can be explained in terms of screening only, resulting in the well-known Mott criterion $\kappa a_0 \sim 1$, where κ is the inverse screening length and a_0 is the exciton Bohr radius. In contrast, in one and two dimensions such a criterion is rather meaningless since bound states occur for infinitesimal attractive interactions, and, moreover, the fluctuation effects invalidate the concept of random-phase-approximation (RPA) -type screening [in two dimensions (2D) this has been discussed in Ref. 5]. The unbinding of the exciton is, in this case, mainly a consequence of the blocking of the states available for binding, leading to the low-temperature criterion $k_F a_0 \sim 1$, where k_F is the Fermi wave number. Note that this picture already explains some of the phenomena observed in QW. We are referring to the fact that at temperatures $T < \varepsilon_F$ (ε_F is the Fermi energy), in n -type samples the $n=1$ hh (heavy hole) and lh (light hole) atomic excitons disappear at approximately the same density, while in the p -type case the $n=1$ hh exciton unbinds first. Similar conclusions can be drawn from the behavior of the $n=2$ hh exciton.^{1,6}

Even though atomic bound states are no longer stable, within the “rigid Fermi-sea” picture a bound state with respect to the Fermi level still exists. This state was first discussed by Mahan⁷ and we shall refer to it as the “Mahan exciton.” Formally, it is equivalent to loosely bound Cooper pairs in superconductors. As already noted by Mahan, such a bound state in the continuum must eventually shift and broaden as a result of interactions with particle-hole excitations of the Fermi sea. However, to accomplish this “unbinding of the Mahan exciton” one must allow for the dynamical response of the Fermi surface to the appearance (or disappearance) of the hole in the course of optical transitions.

III. INFINITE HOLE MASS CASE— THE X-RAY PROBLEM

Including the full dynamical response of the Fermi sea in a detailed calculation of optical spectra represents a highly nontrivial task, outside the scope of conventional perturbation theory, as discussed qualitatively by Gavoret *et al.*⁸ The easiest way to understand the origin of the difficulty is to consider the optical process in the idealized limit of an infinite hole mass, in analogy with the discussion of the soft x-ray spectra of metals.

There are two effects one must consider: The first was discussed in the pioneering work of Mahan,⁹ who showed that by considering all processes which involve repeated scattering of an electron and a hole, including the vertex corrections ignored within the static Fermi-sea picture (backward scattering), the sharp bound state at the Fermi level changes into a power-law singularity. The second effect is related to the “orthogonality catastrophe” dis-

cussed by Anderson¹⁰ and Hopfield.¹¹ Anderson proved that the overlap between the electron ground-state wave function in the absence of the hole and that with the hole present vanishes in the limit of a large system. As a result of this effect alone, the absorption spectrum would be nonvanishing only away from the Fermi level, since in that case, due to the creation of particle-hole pairs, the final state would be an excited state, not affected by Anderson’s theorem. (Formally, the orthogonality theorem is contained in the hole self-energy.) The singularity due to the “final-state interactions” discussed by Mahan usually dominates, and thus the absorption spectrum (in the absence of atomic excitons) displays a power-law singularity at the Fermi level.

The main physical points of the above discussion can be clarified by considering a simple model in which a spin-down electron is photoexcited above the Fermi level, leaving behind a localized hole with spin up ($m_s = +\frac{1}{2}$) and energy E_g , coupled through contact direct (U) and exchange (J) interactions to the Fermi sea of $N+1$ electrons. The Hamiltonian of the final state (f) defined in the course of the absorption process is

$$H_f = E_g + \sum_{k,s} \varepsilon_e(k) a_{k,s}^\dagger a_{k,s} - \frac{U}{N} \sum_{k,k',s} a_{k,s}^\dagger a_{k',s} - \frac{J}{4N} \sum_{k,k',s,s'} a_{k,s}^\dagger \tau_z^{ss'} a_{k',s'}, \quad (1)$$

where $a_{k,s}$ ($a_{k,s}^\dagger$) are annihilation (creation) operators for spin $m_s = \pm \frac{1}{2}$ electrons, $\varepsilon_e(k)$ is the conduction electron (single-particle) energy, and τ_z is the diagonal Pauli matrix. The initial state (i) consists solely of the unperturbed Fermi sea (of N electrons). [We note that the behavior discussed in the preceding paragraph is independent of the details of the electron-hole interaction (provided it is short ranged) and thus the simple model implied by (1) is sufficient for our purposes.] For a constant dipole matrix element, M , the absorption rate $I(\omega)$ can be obtained from the correlation function

$$W(t) = \frac{1}{N} \sum_{k,k'} \langle i | e^{iH_i t} a_{k,i} e^{-iH_f t} a_{k',i}^\dagger | i \rangle, \quad (2)$$

$$I(\omega) = \text{Im}(i | M |^2 / \pi) \int dt e^{i\omega t} W(t).$$

The calculation of the absorption rate $I(\omega)$ close to the threshold becomes trivial if we adopt the picture introduced by Schotte and Schotte¹² in their discussion of the x-ray problem. By considering s -wave scattering only [as implied in (1)] Schotte and Schotte replaced the Fermi sea by a one-dimensional electron gas representing the electron degrees of freedom in spherical energy shells about the hole. In the asymptotically weak U and J limit they model the excitations close to the Fermi level in terms of “Tomonaga bosons;” in this picture the appearance of the hole in the course of the absorption process then gives rise to an infinite number of bosonlike charge and spin-density-wave excitations of the Fermi sea. This kind of mapping is limited to systems without bound states and, strictly speaking, does not apply in one and two dimensions (see below). In terms of the corresponding Tomonaga boson operators $b_{k,s}$ ($b_{k,s}^\dagger$) the Hamiltonians H_i and

H_f and the fermion operator $(1/\sqrt{N})\sum_k a_{k,1}$ in (2) can be written as

$$H_i = \sum_{k,s} \frac{k}{\rho} b_{k,s}^\dagger b_{k,s} + C_i, \quad (3a)$$

$$H_f = \sum_{k,s} \frac{k}{\rho} \left[b_{k,s}^\dagger - \frac{\rho W_s}{\sqrt{Nk}} \right] \left[b_{k,s} - \frac{\rho W_s}{\sqrt{Nk}} \right] + C_f, \quad (3b)$$

$$\frac{1}{\sqrt{N}} \sum_k a_{k,1} \sim \exp \sum_k \frac{1}{\sqrt{Nk}} (b_{k,1}^\dagger - b_{k,1}). \quad (3c)$$

Above, $W_s = U + Jm_s/2$ and ρ is the conduction electron density of states at the Fermi level; C_i and C_f are constants; the wave vector $k = |k|$ indexes the energy shells.

As already alluded to, the Hamiltonian (3) only treats explicitly the excitations of the Fermi sea and does not, of course, describe the binding of electrons and holes into excitons. These can be allowed for by adding an orthogonal bound state contribution to the scattering state given in (3c). The extrapolation to strong coupling as well as the correct electronic energies [denoted by constants in (3)] can be obtained by trivially extending both the Friedel sum rule¹³ and Fumi's theorem¹⁴ to include bound states. The final results are parametrized in terms of the exact scattering phase shifts, $\delta_s(\omega)$.

The absorption spectrum as defined in (2) has the form

$$I(\omega) \sim A(\omega - \omega_1)^{-\alpha_1} + B(\omega - \omega_2)^{-\alpha_2},$$

first obtained by Combescot and Nozières.¹⁵ The two threshold energies, ω_1 and ω_2 , follow directly from Eq. (2) and are given by

$$\omega_{1,2} = \min(E_f^{N+1} - E_f^N) + (E_f^N - E_i^N) + E_g,$$

where E_i^N and E_f^N are the ground-state electronic energies in the initial and final state, respectively. In the Schotte-Schotte model the exponents $\alpha_{1,2}$ are calculated in terms of the Born approximation scattering phase shifts at the Fermi level (in spin channel s), $\delta_s(\epsilon_F) = \pi\rho W_s$. The energies are obtained from Fumi's theorem, $E_f^N - E_i^N = -\sum_s \int_0^{\epsilon_F} d\omega \delta_s(\omega)/\pi$. One finds a primary threshold at the absolute minimum of $(E_f^{N+1} - E_f^N) = -E_0$, the binding energy of the singlet exciton, and a secondary threshold at $\min(E_f^{N+1} - E_f^N) = \epsilon_F$, corresponding to the onset of continuum absorption. It is important to note that in the presence of bound states the results given above must be suitably reinterpreted in terms of the scattering phase shifts $\delta'_s = \delta_s - \pi$, which enter the Friedel sum rule. The shift by π exactly corresponds to the number of bound states (one) present in each spin channel. The exponents $\alpha_{1,2}$ are then in agreement with Hopfield's rule of thumb¹¹ and can be written in terms of the number of electrons, $n_{s;1,2}$, required to screen the hole potential in the $m_s = \pm \frac{1}{2}$ channels

$$\alpha_{1,2} = 1 - \sum_s (n_{s;1,2})^2. \quad (4)$$

According to these considerations, the primary threshold in the presence of atomic bound states is situated at

$$\omega_1 = E_g - E_0 - \sum_s \int_0^{\epsilon_F} d\omega [\delta_s(\omega)/\pi - 1]$$

and has an exponent $\alpha_1 = 1 - \sum_s [\delta_s(\epsilon_F)/\pi - 1]^2$. This corresponds to an absorption process in the course of which both a spin-up and a spin-down electron are bound; thus, only $\delta_s(\epsilon_F)/\pi - 1 = \delta'_s(\epsilon_F)/\pi$ electrons are required to screen the hole in each channel. While the spin-up electron is always bound and inaccessible in optical transitions, the bound spin-down electron can be thought of as originating from the absorption process. In the low-doping limit $\epsilon_F \rightarrow 0, \delta_s(\epsilon_F) \rightarrow \pi$ and we recover a δ -function absorption line ($\alpha_1 \rightarrow 1$) at the singlet exciton position. In this same limit, the secondary threshold is situated at

$$\omega_2 = E_g + \epsilon_F - \sum_s \int_0^{\epsilon_F} d\omega [\delta_s(\omega)/\pi - 1]$$

and is characterized by an exponent $\alpha_2 = 1 - [\delta_1(\epsilon_F)/\pi - 1]^2 - [\delta_1(\epsilon_F)/\pi - 2]^2$. Clearly, the counting is unchanged for the spin-up electrons; however, the spin-down electron in the singlet bound state and the spin-down electron originating from the absorption process are now distinct and thus only $\delta_1(\epsilon_F)/\pi - 2$ electrons in the Fermi sea are required for the screening of the hole potential in the \downarrow channel. In the low-doping limit $\alpha_2 \rightarrow 0$, and the secondary threshold corresponds to the usual continuum edge E_g including the Sommerfeld enhancement [Fig. 1(a)].

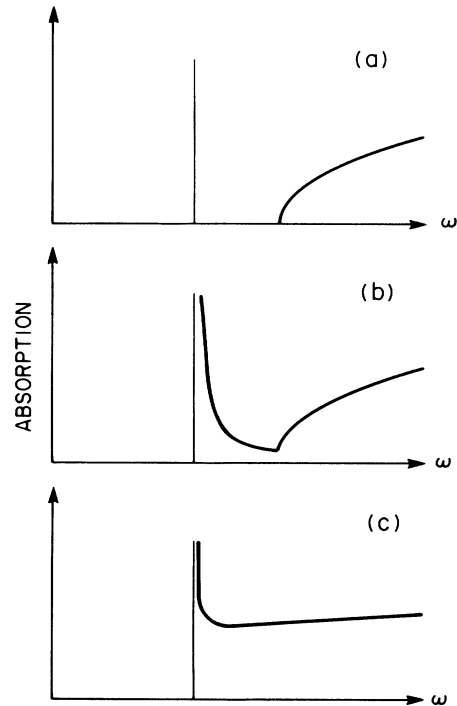


FIG. 1. Qualitative absorption spectra in the infinite hole mass case as a function of doping: (a) undoped case; (b) low-doping concentrations; (c) high doping concentrations ($k_F a_0 \gg 1$). We have displaced the spectra so that they all have the same primary threshold, ω_1 ; the density of states is not meant to mimic a particular single-particle band structure.

With increasing doping the primary threshold broadens [Fig. 1(b)]. Even though a complete analytical calculation of this behavior is not yet available (see, however, below), we argue on physical grounds that in any dimension the primary threshold changes continuously from the exciton dressed with an infinite number of charge and spin-density wave excitations in the low-doping limit to the Fermi-level singularity in the weak-coupling, high-doping limit, $\delta_s(\epsilon_F) \rightarrow 0$ [Fig. 1(c)]. In the latter case the results of the preceding paragraph can be carried over by replacing $\delta'_s(\omega) = \delta_s(\omega) - \pi$ by $\delta'_s(\omega) = \delta_s(\omega)$, the phase shift in the absence of bound states, which is now correctly given by the Born approximation, $\delta_s = \pi \rho W_s$, as calculated in the Schotte-Schotte model.¹² (It is worth noting that since we insist on parametrizing the results in terms of two-particle scattering phase shifts, we are forced to reinterpret the phase shifts discontinuously once atomic excitons unbind.)

IV. FINITE HOLE-MASS AND THE INDIRECT THRESHOLD

In the case of a finite hole mass, the recoil of the hole will smear the Fermi-level singularity over a frequency range $(m_e/m_h)\epsilon_F$, the effective "bandwidth" of the hole, m_e and m_h being the electron and hole effective masses. In this case, optical processes can be separated into two categories, direct and indirect (Auger-like) transitions. In the high-doping limit, direct transitions (which correspond to the excitation of an electron and a hole with wave vectors k and $-k$, respectively) require a minimum energy $\omega_D = E_g + (1 + m_e/m_h)\epsilon_F$ (Fig. 2); while in indirect transitions electrons are excited above the Fermi level

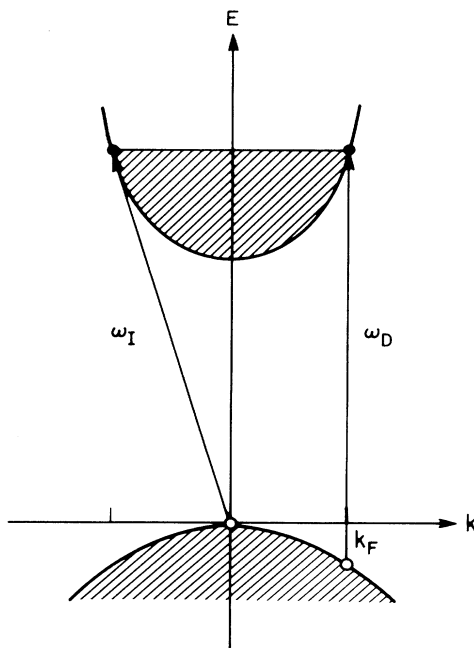


FIG. 2. Direct (with threshold ω_D) and indirect (with threshold ω_I) absorption processes for a finite hole mass.

under the simultaneous excitation of particle-hole pairs or plasmons, which ensure energy and momentum conservation. As can be seen from Fig. 2, the indirect threshold (i.e., the minimum energy required for such a process) is given by $\omega_I = E_g + \epsilon_F$. When the recoil energy, $\omega_D - \omega_I$, is much larger than the Coulomb energy (as measured by the binding energy of the Mahan exciton) the structure at the Fermi level disappears completely [Fig. 3(a)]; in the opposite limit there is a broadened resonance which survives between the two thresholds and which, in the limit of infinite hole mass, develops into the x-ray singularity [Fig. 3(b)]. Above, E_g and the effective masses have to be suitably interpreted in terms of the renormalized energy gap and mean effective masses (between $k=0$ and $k=k_F$), as determined from the single-particle self-energies. In the low-doping, atomic-exciton limit, the recoil of the hole plays a minor role and the line shape is qualitatively the same as that for an infinite hole mass [Figs. 1(a) and 1(b)].

Unfortunately, and as explained below, very little can actually be calculated analytically in the case of a finite hole mass, except for the behavior near the indirect threshold, which can be obtained from conventional perturbation theory. A previous calculation of the indirect threshold⁸ was based on a quasiparticle picture for the conduction electrons which, however, breaks down away from the Fermi level.

Clearly, a fully quantitative treatment does require that, to a given order in the screened Coulomb interaction, both electron and hole self-energies and vertex corrections, be treated on equal footing. All contributions to the indirect threshold, up to second order in the dynamically screened Coulomb interactions, are given in Fig. 4; Figs. 4(a) and 4(b) are due to the direct and exchange parts of the conduction electron self-energy; Fig. 4(c) is due to the hole self-energy, and 4(d), 4(e), and 4(f) are due to the corre-

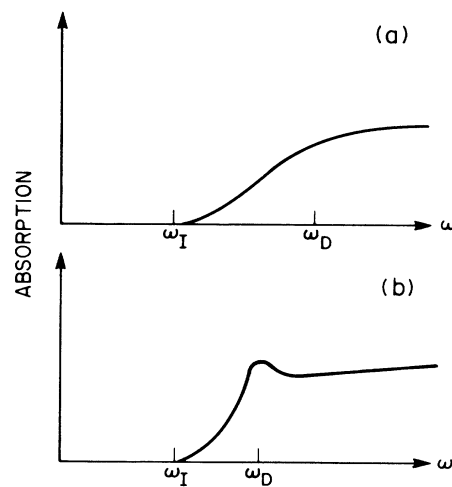


FIG. 3. Qualitative absorption spectra in the finite hole mass case at high doping concentrations ($k_F a_0 \gg 1$) for (a) $\omega_D - \omega_I \gg E_M$ [$E_M \sim (m_e \epsilon_F / m) \exp(-m_e / m \rho U)$ is the binding energy of the "Mahan exciton," where m is the reduced electron-hole mass]; (b) $\omega_D - \omega_I \sim E_M$.

sponding vertex corrections, respectively. These diagrams represent the photon self-energy, $\Pi(q \approx 0, z)$, the imaginary part of which determines, respectively, the absorption and emission spectra, $I(\omega) \sim -\text{Im}\Pi(q \approx 0, \omega + i0)$ and $L(\omega) \sim I(\omega)\{\exp[\beta(\omega - \mu)] - 1\}^{-1}$, where μ is the quasichemical potential for electron-hole pairs, and β is the inverse temperature $(k_B T)^{-1}$. The direct evaluation

of the diagrams is tedious but straightforward. The results are, however, intuitive and can also be obtained by a simple ‘‘cutting’’ procedure which leads to a one-to-one correspondence between the diagrams and conventional second-order perturbation theory.

The final expression for $I(\omega)$ and the low-energy tail of $L(\omega)$ read

$$I(\omega) = \sum_{k,k',k''} M(k,k',\omega)[2M^*(k,k',\omega) - M^*(k,k'',\omega)](1-f_{e,k'})(1-f_{e,k''})f_{e,k''+k'-k} \times \delta(\omega - E_{h,-k} - E_{e,k'} - E_{e,k''} + E_{e,k''+k'-k}), \quad (5a)$$

$$L(\omega) = \sum_{k,k',k''} M(k,k',\omega)[2M^*(k,k',\omega) - M^*(k,k'',\omega)]f_{e,k'}f_{e,k''}(1-f_{e,k''+k'-k}) \times f_{h,-k}\delta(\omega - E_{h,-k} - E_{e,k'} - E_{e,k''} + E_{e,k''+k'-k}), \quad (5b)$$

where the effective matrix element $M(k,k',\omega)$ is given by

$$M(k,k',\omega) = MU(k-k',\omega - E_{h,-k} - E_{e,k'}) \left[\frac{1}{\omega - E_{h,-k} - E_{e,k}} - \frac{1}{\omega - E_{h,-k'} - E_{e,k'}} \right]. \quad (6)$$

M is the optical matrix element (here assumed constant), $E_{i,k}$ and $f_{i,k}$, $i=e,h$, are the (renormalized) single-particle energies and distribution functions for electrons and holes, and $U(q,\omega)$ is the retarded, dynamically screened Coulomb interaction. Equation (5) can be trivially extended to allow for electron-hole exchange, in which case the two denominators in (6) have different coefficients.¹ We note that to leading order in the detuning, $\omega - \omega_I$, the two- and three-dimensional absorption spectra, $I_2(\omega)$ and $I_3(\omega)$, reduce to

$$I_2(\omega) = (2\pi\sqrt{3})^{-1} \left[1 + \frac{m_e}{m_h} \right] |M_2 U_2(k_F, 0)|^2 \rho_2^3 \times \left[\frac{\omega - \omega_I}{k_F^2/2m_h} \right]^3, \quad (7a)$$

$$I_3(\omega) = \frac{1}{15} \left[1 + \frac{m_e}{m_h} \right] |M_3 U_3(k_F, 0)|^2 \rho_3^3 \times \left[\frac{\omega - \omega_I}{k_F^2/2m_h} \right]^{7/2}, \quad (7b)$$

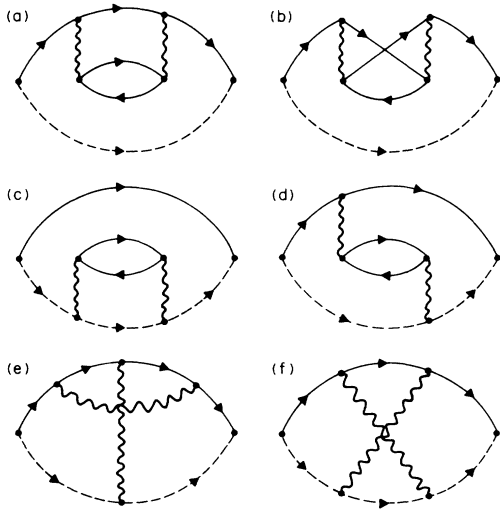


FIG. 4. Second-order diagrams contributing to the indirect threshold. Wiggly, solid, and dashed lines represent the screened Coulomb interaction, electron and hole propagators, respectively.

where ρ is the conduction electron density of states at the Fermi level ($\rho_2 = m_e/2\pi, \rho_3 = m_e k_F/2\pi^2$).

There are several comments to be made concerning these expressions. First notice the partial cancellation between direct $[2M^*(k,k',\omega)]$ and exchange $[M^*(k,k'',\omega)]$ contributions in (5a) and (5b) for momentum transfer k_F , a consequence of the exchange hole surrounding each electron. It is also noteworthy that, again due to the large momentum transfer, self-energy and vertex corrections add at the indirect threshold, rather than subtract as in the case of small momentum transfer (where the cancellation reflects charge neutrality). As apparent from (7), the contributions from the electron-electron interaction, which were left out in Ref. 8, lead to corrections of order m_e/m_h and thus cannot be ignored in general. Finally, in expressions (5) the full dynamically screened Coulomb interaction enters, and thus plasmon emission and absorption processes are naturally included. Near the indirect absorption threshold these are irrelevant due to the large momentum transfer, k_F , while in emission they always contribute.

At the direct threshold expressions (5) diverge, reflecting the breakdown of conventional perturbation theory.

As discussed qualitatively in Ref. 8, the cure of this divergence requires a nontrivial self-consistent renormalization of both, single-particle self-energies and vertex function, using the self-consistent “parquet” equations derived in Refs. 16 and 17. This procedure is exact in a sense which we will clarify in the following section. However, the discussion given in Ref. 8 is limited solely to those processes which, for infinite hole mass, lead to the qualitatively correct threshold behavior. For finite hole mass the approach in terms of parquet diagrams has not yet been carried out quantitatively nor has it, so far, been sufficiently motivated from a physical standpoint. Below we suggest an approach based on the solution of the three-particle problem, which (i) clarifies the physics underlying the parquet treatment, and (ii) would allow for a consistent (numerical) calculation of the spectra for arbitrary electron-to-hole mass ratio. A simple model calculation will be presented elsewhere.¹⁸

V. THE THREE-BODY PROBLEM

Any calculation of the optical spectra has to describe correctly (i) the final state interaction and (ii) the remnant of the “orthogonality catastrophe” for a finite mass hole. The latter constitutes the conceptually simple part of the problem and, qualitatively, can be calculated either within the Schotte-Schotte model,¹⁹ or by using the cluster expansion for the hole Green’s function.²⁰ Physically, the relevant processes involve the successive emission of particle-hole pairs which, in the case of a finite hole mass, leads to the renormalization of the hole hopping amplitude. The final-state interaction effects can not be understood as simply; the main problem obviously is to “unbind the Mahan exciton” which occurs in the rigid Fermi-sea picture as a result of the sharpness of the Fermi surface. To accomplish this we incorporate the full treatment of three-particle correlations into the calculation of the spectra. The physical motivation for such an approach is based on the idea that the correlation between the photoexcited electron and hole with single particle-hole pair excitations of the Fermi sea leads to the smearing of the Mahan exciton as a result of the indistinguishability of the two electrons (photoexcited and virtual).

The process implied above, which determines the exact electron-hole scattering amplitude, can be written symbolically as $G_2 = G_{1e}G_{1h} + UG_{1h}G_3$ and is represented graphically in Fig. 5; G_{1e} and G_{1h} are the electron and hole single-particle Green’s functions, and G_3 is the three-particle Green’s function. For the sake of simplicity we consider only a spin-independent electron-hole interaction U , and neglect all electron-electron interactions. To clarify the meaning of this diagram we begin by treating a simple three-particle problem, where two electrons (1 and 3) interact with a (valence band) hole (2) through interactions U_{12} and U_{23} . G_3 is then determined by the three-body Lippmann-Schwinger equation, $G_3 = G_3^{(0)} + G_3^{(0)}(U_{12} + U_{23})G_3$. The kernel of this equation is, however, not compact,⁴ because it contains δ functions associated with the free propagation of one of the electrons, and becomes tractable only by first solving exactly the two-particle problems in each channel. Following Fadeev,

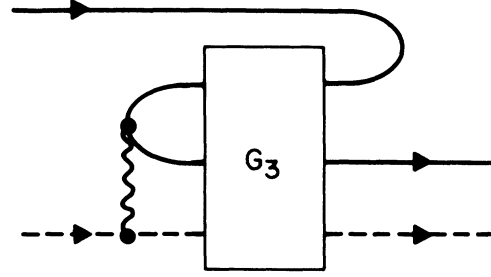


FIG. 5. The connected part of the two-particle Green’s function, G_2 , in terms of the three-particle Green’s function, G_3 .

we first decompose $G_3 = G_3^{(0)} + G_{12} + G_{23}$ which leads to the equations

$$G_{12} = G_3^{(0)} U_{12} (G_3^{(0)} + G_{12} + G_{23}), \quad (8a)$$

$$G_{23} = G_3^{(0)} U_{23} (G_3^{(0)} + G_{12} + G_{23}). \quad (8b)$$

The exact solution of the corresponding two-particle problems introduces the disconnected three-particle Green’s functions

$$G_{12}^{(0)} = G_3^{(0)} + G_3^{(0)} U_{12} G_{12}^{(0)}, \quad (9a)$$

$$G_{23}^{(0)} = G_3^{(0)} + G_3^{(0)} U_{23} G_{23}^{(0)}. \quad (9b)$$

From (8) and (9) we finally obtain Fadeev’s equations in the form²¹

$$G_{12} = G_{12}^{(0)} - G_3^{(0)} + G_{12}^{(0)} U_{12} G_{23}, \quad (10a)$$

$$G_{23} = G_{23}^{(0)} - G_3^{(0)} + G_{23}^{(0)} U_{23} G_{12}. \quad (10b)$$

Note that substituting the *disconnected* three-particle Green’s function (with one of the electrons replaced by a freely moving virtual hole) into the diagram in Fig. 5 (or into the equivalent equation for the electron-hole Green’s function, G_2) immediately leads to the Schrödinger equation for the atomic exciton; and in the high-density limit to that for the Mahan exciton.

A treatment of the full three-body problem in the presence of the Fermi sea requires a generalization of the Fadeev equations to include self-energy and vertex renormalization. This can be achieved by closing the hierarchy of the many-body Green’s function equations at the level of the three-particle correlations as explained, for example, by de Dominicis and Martin.²² Without a rigorous derivation we can already note that the Fadeev equations (8a) and (8b) are precisely the same as the parquet equations derived in Ref. 16, if U_{12} and U_{23} are identified with the exact irreducible interactions in the 23 and 12 channels, respectively. In the infinite hole mass case the above treatment thus yields the correct final-state interaction contribution to the x-ray edge singularity.¹⁶ Moreover, this approach also allows for an appealing physical interpretation of the parquet analysis, which was originally introduced solely to account for the most divergent terms in perturbation theory. Ultimately, our aim is to consider the full many-body equations within the framework of the Fadeev approach and develop a quantitative

theory of the optical spectra of doped semiconductors for arbitrary electron-to-hole mass ratio.

VI. CONCLUSIONS

Above, we have described the main aspects of the many-body physics which determine the optical spectra of doped semiconductors with particular emphasis on the breakdown of conventional perturbation theory. We have demonstrated that the simplest theory must be based on a consistent treatment of three-particle correlations, as described by suitably modified Fadeev equations. Such a theory simultaneously accounts for both indirect and direct optical transitions and, in the limit of an infinite hole mass, yields the exact results discussed in the context of the x-ray problem. This discussion is particularly important in view of two recent attempts^{23,24} to calculate the optical spectra of modulation-doped semiconductor quantum wells. In an oversimplified calculation, Bauer and Ando²³ find the singularity associated with the Mahan ex-

citon, which they then remove by hand using inappropriate arguments. On the other hand, even though they recognize the basic difficulty with the straightforward perturbative approach, Chang and Sanders²⁴ fail to include the configuration with the hole in the presence of a relaxed Fermi sea in the initial state, and restrict themselves to *perturbative* intermediate states with a single virtual particle-hole pair, their calculation is thus at best incomplete.

ACKNOWLEDGMENTS

We would like to thank R. C. Miller for collaboration and discussion of experiments, and O. Munteanu, J. C. Phillips, A. Pinczuk, and especially L. J. Sham for useful comments. A. E. Ruckenstein was partially supported by the U.S. Office of Naval Research (ONR). This work was done in part while A.E.R. was a visitor at AT&T Bell Laboratories. He thanks the technical staff at AT&T Bell Laboratories for their hospitality.

¹A. E. Ruckenstein, S. Schmitt-Rink, and R. C. Miller, Phys. Rev. Lett. **56**, 504 (1986).

²R. Sooryakumar, D. S. Chemla, A. Pinczuk, A. Gossard, W. Wiegmann, and L. J. Sham, Solid State Commun. **54**, 859 (1985).

³R. Baltrameyunas, E. Kukshtis, and G. Tamulaitis, Fiz. Tverd. Tela **27**, 3672 (1985) [Sov. Phys.—Solid State **27**, 2211 (1986)].

⁴L. D. Fadeev, *Mathematical Aspects of the Three-Body Problem in Quantum Scattering Theory* (Davey, New York, 1965).

⁵S. Schmitt-Rink, in Proceedings of the National Science Foundation Workshop on Optical, Nonlinearities, Fast Phenomena and Signal Processing, Tucson, 1986 (unpublished).

⁶R. C. Miller and D. A. Kleinman, J. Lumin. **30**, 520 (1985).

⁷G. D. Mahan, Phys. Rev. **153**, 882 (1967).

⁸J. Gavoret, P. Nozières, B. Roulet, and M. Combescot, J. Phys. (Paris) **30**, 987 (1969).

⁹G. D. Mahan, Phys. Rev. **163**, 612 (1967).

¹⁰P. W. Anderson, Phys. Rev. Lett. **18**, 1049 (1967).

¹¹J. Hopfield, Comments Solid State Phys. **2**, 40 (1969).

¹²K. D. Schotte and U. Schotte, Phys. Rev. **182**, 479 (1969).

¹³J. Friedel, Philos. Mag. **43**, 153 (1952).

¹⁴F. G. Fumi, Philos. Mag. **46**, 1007 (1955).

¹⁵M. Combescot and P. Nozières, J. Phys. (Paris) **32**, 913 (1971).

¹⁶B. Roulet, J. Gavoret, and P. Nozières, Phys. Rev. **178**, 1072 (1969); P. Nozières, J. Gavoret, and B. Roulet, Phys. Rev. **178**, 1084 (1969).

¹⁷P. Nozières and C. T. de Dominicis, Phys. Rev. **178**, 1097 (1969).

¹⁸A. E. Ruckenstein, and S. Schmitt-Rink (unpublished).

¹⁹E. Muller-Hartmann, T. V. Ramakrishnan, and G. Toulouse, Phys. Rev. B **3**, 1102 (1971).

²⁰S. Doniach, Phys. Rev. B **2**, 3898 (1970).

²¹W. Glockle, *The Quantum Mechanical Few-Body Problem* (Springer, New York, 1983).

²²C. de Dominicis and P. C. Martin, J. Math. Phys. **5**, 14 (1964).

²³G. E. W. Bauer and T. Ando, Phys. Rev. B **31**, 8321 (1985).

²⁴Y. C. Chang and G. D. Sanders, Phys. Rev. B **32**, 5521 (1985).